

# PROCEEDINGS OF SPIE

[SPIDigitalLibrary.org/conference-proceedings-of-spie](https://SPIDigitalLibrary.org/conference-proceedings-of-spie)

## Synthesis and characterization of semiconducting oxide nanoparticles and hybrid composites with energy-related applications

Vázquez-López, Antonio, García-Alonso, Javier, Nahirniak, Svitlana, Bartolomé, Javier, Ramírez-Castellanos, Julio, et al.

Antonio Vázquez-López, Javier García-Alonso, Svitlana Nahirniak, Javier Bartolomé, Julio Ramírez-Castellanos, David Maestre, Bilge Saruhan, Ana Cremades, "Synthesis and characterization of semiconducting oxide nanoparticles and hybrid composites with energy-related applications," Proc. SPIE 12002, Oxide-based Materials and Devices XIII, 120020F (5 March 2022); doi: 10.1117/12.2619378

**SPIE.**

Event: SPIE OPTO, 2022, San Francisco, California, United States

# Synthesis and characterization of semiconducting oxide nanoparticles and hybrid composites with energy-related applications

Antonio Vázquez-López<sup>a</sup>, Javier García-Alonso<sup>a</sup>, Svitlana Nahirniak<sup>b</sup>, Javier Bartolomé<sup>a,c</sup>, Julio Ramírez-Castellanos<sup>d</sup>, David Maestre<sup>\*a</sup>, Bilge Saruhan<sup>b</sup>, Ana Cremades<sup>a</sup>

<sup>a</sup>Departamento de Física de Materiales, Facultad de CC. Físicas, Universidad Complutense de Madrid, 28040, Spain ; <sup>b</sup>Institute of Materials Research, German Aerospace Center (DLR), Linder Hoehe 51147, Cologne, Germany ; <sup>c</sup>Departamento de Física Aplicada, Facultad de Ciencias, Universidad Autónoma de Madrid, 28049, Spain ; <sup>d</sup>Departamento de Química Inorgánica, Facultad de CC. Químicas, Universidad Complutense de Madrid, 28040, Spain

## ABSTRACT

The advent of modern devices requires the development of multifunctional nanomaterials with improved performance, while involving low-cost and sustainable processing. In this frame semiconducting oxide nanoparticles and hybrid composites formed by their combination with an organic matrix are gaining increasing attention based on their versatility and wide range of applicability in many fields of technological research. In this work semiconducting oxide nanoparticles (SnO, SnO<sub>2</sub>, TiO<sub>2</sub>, Ni-Mn-O) and hybrid composites formed with the nanoparticles embedded in Poly(3,4-ethylene-dioxythiophene)-poly(styrenesulfonate) (PEDOT:PSS) have been synthesized following diverse chemical routes. The samples have been characterized by using advanced microscopy and spectroscopy techniques and their performance in photovoltaics, thermoelectrics, gas sensing, and energy-related applications have been evaluated. Improvements were achieved by the synergy between the components of the composites.

**Keywords:** semiconducting oxide, nanoparticles, hybrid composite, thermoelectrics, gas sensing

## INTRODUCTION

During the last years, great improvements have been achieved in the synthesis of semiconducting oxide nanostructures with controlled dimensions, morphology and tailored properties,<sup>1-3</sup> while broadening their applicability in a growing number of technological fields of research, such as photovoltaics, sensors, photocatalysts, thermoelectrics, and energy storage and harvesting, to name a few. In addition to binary oxides, more complex oxide-based compounds have been also explored in order to optimize and widen their plethora of applications.<sup>4</sup> Their inherent versatility makes these materials of prior choice in the design of multifunctional devices, including energy-related applications. Besides, hybrid composites combining organic and inorganic nanomaterials have recently become of great interest based on the improved properties derived from the synergy between their components which can lead to flexible, low-cost, and scalable devices with good stability and tunable electrical and optical properties. Carbonaceous materials, including graphene and graphene oxide, and polymeric materials, have been commonly used as matrix in which semiconducting oxide nanostructures act as fillers. These hybrid composites are called to revolutionize many technological fields of research, including energy-related applications such as solar cells,<sup>5</sup> thermoelectrics,<sup>6</sup> or sensors.<sup>7</sup>

In this work, diverse p-type (SnO) and n-type (SnO<sub>2</sub>, anatase-TiO<sub>2</sub>) semiconducting oxide nanoparticles have been synthesized following a hydrolysis method and used as fillers in the formation of hybrid composite layers in combination with Poly(3,4-ethylene-dioxythiophene)-poly(styrenesulfonate) (PEDOT:PSS). Moreover, more complex Ni-Mn-oxide based particles were synthesized following a co-precipitation route and studied in the search of improved cathode materials in Li-ion batteries (LiBs). The potential applicability of the semiconducting oxide nanoparticles and the hybrid layers, deposited via spin coating onto glass or Si substrates, have been evaluated in photovoltaic, thermoelectrics and energy-related applications in order to get deeper insights in the understanding of the physical phenomena governing the analyzed behavior and broaden the versatility of these nanomaterials. This study settles the grounds for the multifunctional applicability of the hybrid composites in diverse energy-related applications.

## EXPERIMENTAL

Semiconducting oxide samples in form of nano- and microparticles have been synthesized following different chemical routes. A soft chemistry route based on hydrolysis was employed for the synthesis of SnO, SnO<sub>2</sub> and TiO<sub>2</sub> nanoparticles, by using selected precursors, as detailed in previous works<sup>8-11</sup>. Hybrid composites were fabricated by mixing controlled concentration of the metal oxide nanoparticles in a PEDOT:PSS polymeric matrix with the addition of different organic solvents such as dimethyl sulfoxide (DMSO) and Triton X-100, as previously described.<sup>8,11</sup> Alternatively to the use of DMSO, also 1% Ethylene glycol (EG) was added in order to enhance the nanoparticles dispersion, leading to an increase in the electrical conductivity as well.<sup>12</sup> The films were deposited either on silicon or glass substrates by spin coating. On the other hand, Ni-Mn oxide particles were synthesized by an oxalate assisted co-precipitation route, which can also lead to the formation of Ni-rich core and Mn-rich shell structures. X-ray diffraction (XRD) in a PANalytical X'Pert Powder equipment using the copper K $\alpha$  line was used for the structural characterization. Scanning and transmission electron microscopy (SEM, TEM) were employed for the morphological study. Energy dispersive x-ray spectroscopy (EDS) measurements were carried out in a SEM (Leica 440 Stereoscan) equipped with a Bruker AXS 4010 analyzer. Optical absorption measurements were performed in a UV-1603 UV-Visible spectrophotometer Simadzu (Izasa Scientific). Raman spectroscopy measurements were acquired in a confocal microscope Horiba Jobin Yvon LabRam HR800 using a He-Ne (633 nm) and He-Cd (325 nm) lasers as excitation sources. Quasi-steady state photoconductance (QSS-PC) was analyzed using a BT imaging LIS-R1 at constant illumination (808 nm). Atomic Force Microscopy (AFM) was measured in a Nanotec AFM controlled by Dulcinea electronics using a Si tip in contact mode, while the WSxM software<sup>13</sup> was used for the analysis of the images. For the electrical characterization, 4-probe Hall effect Ecopia AMP55T HMS-700 system was used equipped with four Au probes. Thermoelectric and sensing measurements were performed using home-setups. For the thermoelectric setup two Peltier modules (TEC1-12706, 12V) and two K-type thermocouples were used in combination with a temperature acquisition card (Adaptative Junio Controller ADJ-48-450-UR) to measure the temperature, and a Keithley 2000 multimeter was used to acquire voltage measurements. The gas sensing measurements were performed using the setup described by M. Taelo et al.<sup>14</sup>

## RESULTS AND DISCUSSION

Semiconducting oxide nanoparticles synthesized by hydrolysis exhibit high crystallinity and good homogeneity in size, with averaged dimensions ranging from 6 nm (anatase TiO<sub>2</sub>) to 10 nm (SnO and SnO<sub>2</sub>), as shown in Figure 1a. XRD measurements, not shown here, demonstrated the high crystallinity of the nanoparticles.<sup>9,11</sup> Controlled amounts of these nanoparticles, between 0.5 and 2 % wt., were used as fillers in a PEDOT:PSS-based matrix and subsequently spin coated onto Si or glass substrates. The spin coated films show homogeneous thickness around 150 nm, as measured by SEM (Figure 1b) and further assessed by measuring an AFM profile of the layer (not shown here). Besides, the films show low averaged surface roughness around 3 nm (Figure 1c), based on the optimized spin coated method and due to the effect of the organic solvents such as DMSO or EG,<sup>15,16</sup> which tend to ease the surface structure of PEDOT:PSS layers towards a more granular-like surface.<sup>17</sup> In this work, the versatility of these hybrid layers has been probed in photovoltaic, thermoelectrics, and gas sensing devices.

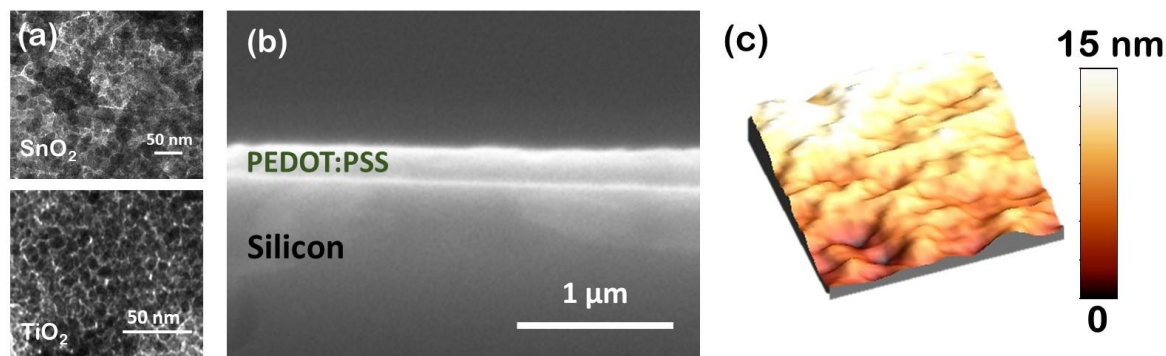


Figure 1. (a) TEM images from SnO<sub>2</sub> and TiO<sub>2</sub> nanoparticles. (b) Cross-sectional SEM image of a PEDOT:PSS layer spin-coated onto a Si substrate. (c) AFM image of a PEDOT:PSS layer.

Firstly, hybrid layers formed by p-type PEDOT:PSS and SnO<sub>2</sub> nanoparticles in variable concentrations (0.5, 1, 2 % wt.) were spin coated onto Si substrates ((100) oriented FZ n-type Si wafer) in order to study their passivation behavior and their potential use in Si-hybrid solar cells, involving low-cost and competitive efficiency. PEDOT:PSS has been regarded as a potential material for this technology.<sup>18,19</sup> In this case, controlled additives, such as Triton X-100 and dimethyl sulfoxide (DMSO) were also added in order to improve the electrical response and dispersion, while preventing degradation. In all cases, the addition of SnO<sub>2</sub> nanoparticles improves the electrical conductivity of the films, reaching values ranging up to  $8.5 \cdot 10^2 \text{ Scm}^{-1}$  for the hybrid composites, while keeping good optical properties in the visible range (Figure 2e). QSS-PC-calibrated PL imaging was used to study the passivation behavior of the hybrid films, as shown in Figure 2a, 2b, 2c. Color bars besides PL images indicate the corresponding charge carrier lifetime values, calculated from the QSS-PC curves as a function of the injection levels (Figure 2d). The addition of nanoparticles leads to lifetime values between 100 and 300  $\mu\text{s}$ . Improved passivation behavior was achieved for the lowest concentration of nanoparticles (0.5 % wt.), as shown in Figure 2a. This passivation effect observed in hybrid composites is commonly related to charge-assisted mechanism, as reported by other authors.<sup>20</sup> Despite the fact that the measured lifetime values are still below the milliseconds range, as commonly reported when using SiN<sub>x</sub>:H or Al<sub>2</sub>O<sub>3</sub> processed using vacuum-assisted or high-temperature procedures,<sup>21</sup> there is still room for improvement in the development of hybrid passivation materials by means of low-cost and easy procedure, as that described in this work. These p-type hybrid layer/n-type Si systems act as p-n junction showing diode-like behavior, as observed in the corresponding I-V curves (Figure 2f), which paves the way to further improvements in the development of hybrid solar cells based on the composites described in this work, as is aligned with the results on similar composites based on other nano-oxides such as Ga<sub>2</sub>O<sub>3</sub>.<sup>22</sup>

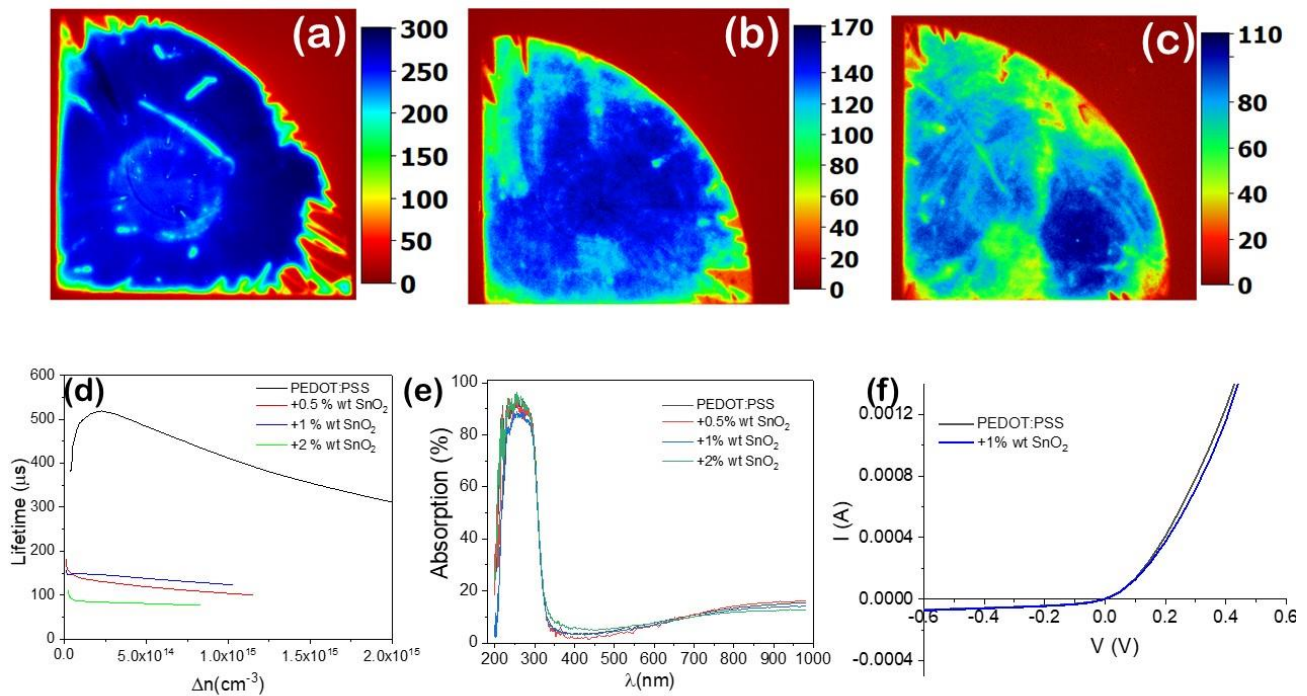


Figure 2. PL images from hybrid composites formed by PEDOT:PSS and (a) 0.5 %, (b) 1 % and (c) 2 % wt. of SnO<sub>2</sub> nanoparticles, and the corresponding (d) QSS-PC curves, (e) optical absorption measurements, and (f) I-V curves from PEDOT:PSS and hybrid composite with SnO<sub>2</sub> nanoparticles in 1 % wt.

Similar composites based on a PEDOT:PSS matrix and the oxide nanoparticles were mixed with Ethylene glycol (EG). The electrical conductivity of the hybrid composites was analyzed at room temperature by the Van der Pauw method, using the adequate Ag contacts configuration. Figure 3a shows a clear increase in the conductivity values ( $\sigma$ ) when adding semiconducting oxide nanoparticles (1 % wt.) to the polymeric matrix. In particular, the use of SnO (p-type) as a filler leads to conductivity values 40 times higher than when using pristine PEDOT:PSS. Some authors associate the conductivity increase with the interaction of the nanoparticles with the PSS-chains.<sup>23</sup> However, the use of

semiconducting oxide nanoparticles slightly reduces the Seebeck coefficient ( $S$ ) of the probed layers (Figure 3a). Based on these values, the corresponding Power Factor can be estimated,  $PF = S^2 \cdot \sigma$  [ $\mu\text{Wm}^{-1}\text{K}^{-2}$ ], as a reference for their thermoelectric behavior. Using SnO nanostructures in a 1 % wt. concentration and EG (1 % wt.) leads to improved thermoelectric performance, with a PF value of  $0.23 \pm 0.01 \mu\text{Wm}^{-1}\text{K}^{-2}$ , more than 30 times higher than pristine PEDOT:PSS layers, while a weak increase in the PF value is achieved when using n-type  $\text{TiO}_2$  nanoparticles (1 % wt.) as a filler (Figure 3b).

In addition, these hybrid composites also exhibit gas sensing behavior under exposure to different analytes. In this work, ethanol gas was used as analyte (200 ppm) and the gas-sensing response of the hybrid layers was tested at room temperature. Figure 3c shows an increase in the resistance of the probed hybrid layers upon ethanol exposure, as expected for a p-type polymer such as PEDOT:PSS. When a reducing gas, such as ethanol, interacts with the oxygen species adsorbed at the surface, electrons are donated to the polymer leading to a decrease in the hole concentration and the consequent resistance increase, although other mechanisms such as the shortening of PEDOT bonds and polymer swelling should be also considered.<sup>15,24</sup> In this case, a saturation value for the resistance is not observed in the curves in Figure 3c owing to the low exposure time used. This sensing response can be modulated as a function of the filler used in the hybrid composite and its concentration. As shown in Figure 3d, the use of different oxide nanoparticles increase the measured sensitivity ( $S$ ),  $S = (R_g - R_0)/R_0$ ,<sup>25,26</sup> where  $R_g$  is the resistance when the sample is exposed to ethanol, and  $R_0$  corresponds to the resistance without ethanol. This value reaches 2.6 % for PEDOT:PSS/SnO composites, and 0.9 % for PEDOT:PSS/ $\text{TiO}_2$  composites, being 13 and 4.5 times higher than the reference pristine PEDOT:PSS composites. It is worth noting that the analyzed sensing response is observed at room temperature, without external power source needed for high temperature response, thus involving energy saving.

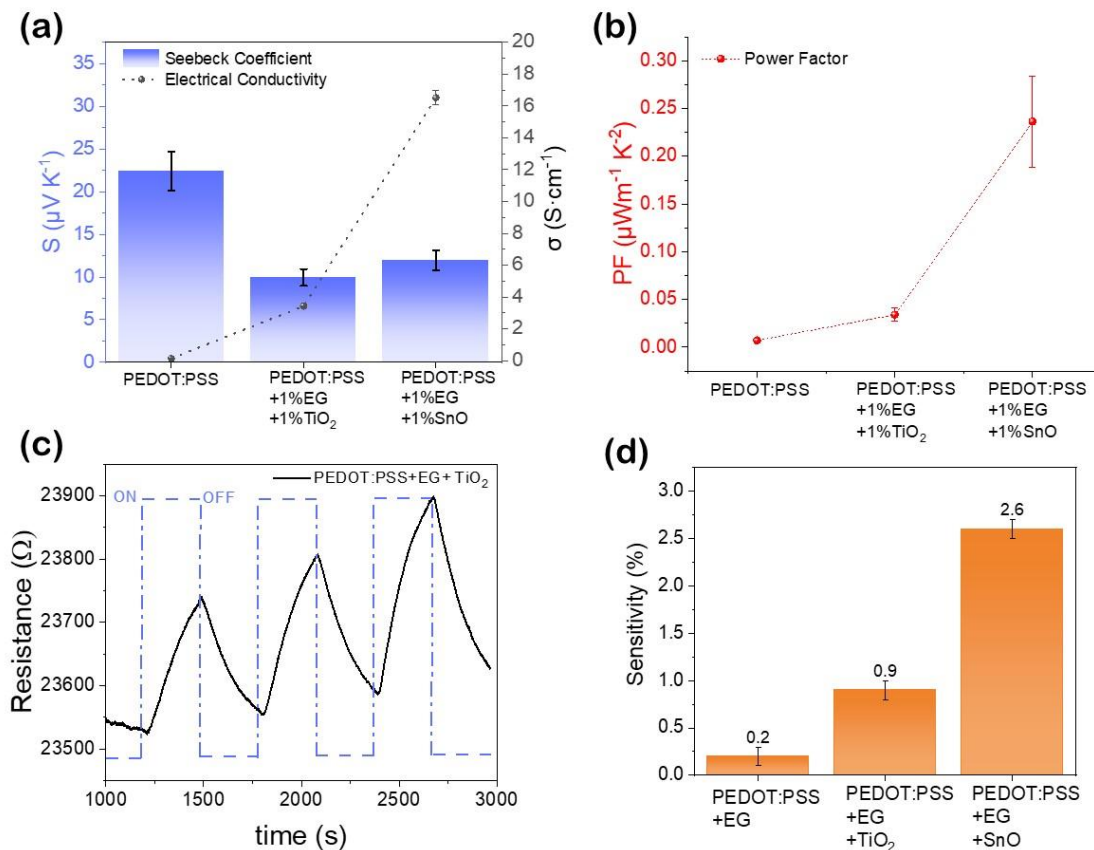


Figure 3. (a) Seebeck coefficient and electrical conductivity values from PEDOT:PSS and composites with  $\text{TiO}_2$  or SnO nanoparticles (1 % wt.). (b) Power Factor values corresponding to the samples in (a). (c) Sensing response from PEDOT:PSS composites with  $\text{TiO}_2$  (1 % wt.) under ethanol exposure, and (d) bar plot showing the sensitivities from diverse hybrid composites.

Finally, these semiconducting oxide nanoparticles have been also used as electrodes in Li-ion batteries (LiBs), based on their good electrochemical behavior, reduced volume expansion, and safe performance, which allows to achieve good capacity and cyclability. In addition to binary oxides, such as  $\text{TiO}_2$  and  $\text{SnO}_2$  nanoparticles which demonstrate good performance as LiBs electrodes,<sup>27,28</sup> more complex oxide-based materials are investigated to overcome some of the actual challenges that face the LiBs. In this frame, NMC-based cathodes have been widely used in LiBs over the last decades due to their high capacity and structural stability. Li-Ni-Mn-Co-O complex oxides are formed by the combination of  $\text{LiMO}_2$  ( $M=\text{Ni, Mn, Co}$ ) that present a layered structure (R-3m).<sup>29</sup> This layered structure allows high capacity and structural stability when NMC is used as cathode material in LIBs. Inside this structure Ni allows for a higher capacity but a lower structural stability when cycling. The presence of Mn allows for higher structural stability but lower capacity. Co in small quantities mitigates the cation disordering inside the crystal structure that can lead to the substitution of Ni cations by Li ions.<sup>30</sup> In this work, NMC particles are analyzed. The Ni-rich core helps to maintain high capacity, while the Mn-rich shell aims to preserve structural stability during LiB performance. The chemical synthesis of core-shell NMC microparticles was achieved in two steps: firstly, synthesis of the core-shell Ni-Mn-Co-O particles by a co-precipitation route, and secondly, Li introduction by a solution evaporation process. Initially, NMC particles, with dimensions around  $4\ \mu\text{m}$ , exhibit a rounded appearance with multiple cracks on the surface and a layered appearance as it can be seen in Figure 4a. The inset in Figure 4a shows a detailed SEM image of an isolated NMC particle. EDS mappings in Figure 4b confirm the compositional homogeneity and the only presence of Ni, Mn, Co and O, within the resolution of the technique (Figure 4d). EDS analysis with variable beam acceleration voltage and at the cracks of the particles confirms the Ni-rich core and a shell with submicrometric dimensions around  $500\ \text{nm}$ . SEM and EDS measurements confirmed that the morphological and compositional properties of the particles were maintained after the Li introduction, despite the weak morphological changes observed at the surface of the particles (Figure 4c). Raman spectroscopy was used to assess the correct introduction of the Li ions inside the particles and the formation of the ternary oxides spinels structures into the NMC R-3m structure. The analysis of the Raman spectra before adding Li (Figure 4e) indicates the formation of different ternary oxides with spinel structure (Fd-3m) at the particles, associated with the two main peaks in Figure 4e, and the possible presence of NiO, central band in Figure 4e. Raman spectra after Li introduction present a band centred at  $500\ \text{cm}^{-1}$  with two clear contributions, the more intense at  $561\ \text{cm}^{-1}$  and a shoulder at lower wavenumbers,  $425\ \text{cm}^{-1}$ . This broad band is characteristic of the layered R-3m structure of NMC.<sup>31</sup> The combination of the distinct  $\text{LiMO}_2$  leads to the superposition of the different Raman modes of these oxides and the observed broad band.

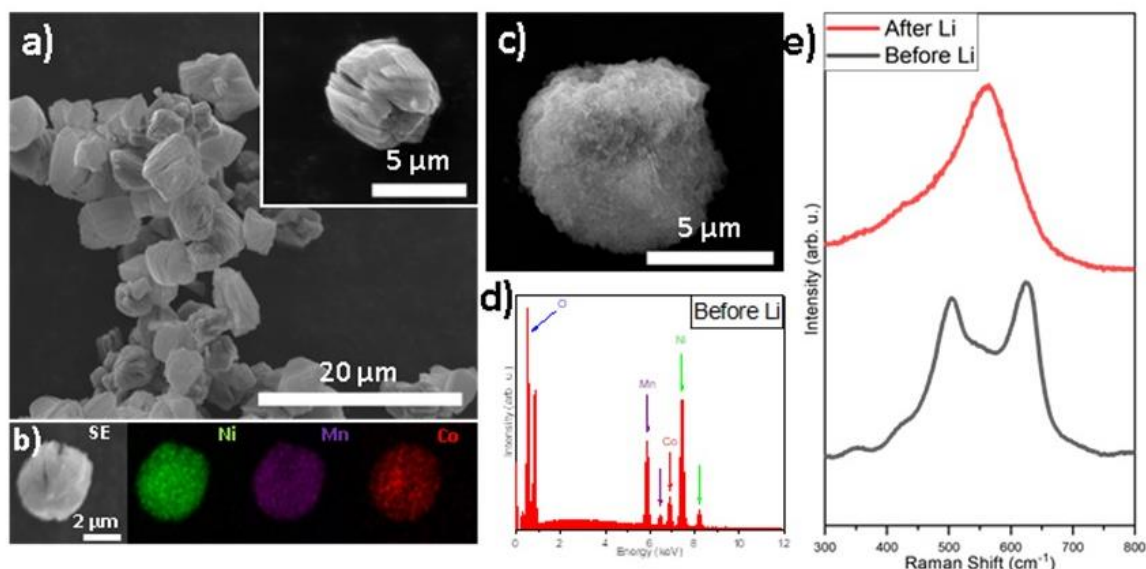


Figure 4. (a) SEM image of NMC particles before adding Li, with a detailed image in the inset. (b) SEM and EDS mappings of a microparticle before adding Li. (c) SEM image of a microparticle after adding Li. (d) EDS spectrum from a microparticle before adding Li. (e) Raman spectra from microparticles before and after adding Li.

## CONCLUSIONS

Semiconducting oxide nanoparticles have been synthesized by different chemical routes and their properties and versatility in different energy-related applications have been investigated. SnO<sub>2</sub>, TiO<sub>2</sub> and SnO nanoparticles with dimensions between 6 – 10 nm were used as fillers in a PEDOT:PSS matrix. The hybrid mixture was spin coated onto glass or Si in order to form layers with thickness around 150 nm. Hybrid composites with low SnO<sub>2</sub> concentration (0.5 % wt.) exhibit good passivation behavior in Si-hybrid solar cells, with carrier lifetime values around 300 μs. Improved thermoelectric response, with PF around 0.2 μWm<sup>-1</sup>K<sup>-2</sup>, was achieved when using SnO (1 % wt.) as a filler in a PEDOT:PSS-based layer. A higher sensitivity to ethanol gas was observed for composites containing either SnO or TiO<sub>2</sub>, with a clear improvement as compared with pristine PEDOT:PSS. Finally, NMC particles as potential material for cathodes in LiBs were investigated before and after adding Li, and only weak morphological changes and variations in the corresponding Raman vibrational modes were observed.

## ACKNOWLEDGEMENTS

This work was funded by the Spanish Ministry of Innovation, Science, and Technology and the Spanish Ministry of Economy through Research Projects RTI2018-097195-B-I00. This research has received funding from the European Union's Horizon 2020 research and innovation programme under Grant Agreement No. 957225, project BAT4EVER.

## REFERENCES

- [1] Guo, T., Yao, M. S., Lin, Y. H. and Nan, C. W., "A comprehensive review on synthesis methods for transition-metal oxide nanostructures," *CrystEngComm* 17(19), 3551–3585 (2015).
- [2] Bartolomé, J., Taelño, M., Vázquez-López, A., Prado, F., García-tecedor, M., Cristian, G., Ramírez-castellanos, J. and Cremades, A., [Oxide-Based Materials and Structures], Taylor and Francis (2020).
- [3] García-Alonso, J., Maestre, D., Bartolomé, J., García-Tecedor, M., Vázquez-López, A., Taelño, M., Prado, F. del, Nogales, E. and Cremades, A., "Synthesis of low dimensional oxide based complex materials by a vapor-solid method," [https://doi.org/10.1117/12.2591251\\_11687](https://doi.org/10.1117/12.2591251_11687), 125–134 (2021).
- [4] Vázquez-López, A., García-Carrión, M., Hall, E., Yaseen, A., Kalafat, I., Taelño, M., Zhu, J., Zhang, X., Arici, E., Taskin, O. S., Maestre, D., Nogales, E., Hidalgo, P., Ramírez-Castellanos, J., Méndez, B., Yuca, N., Karazhanov, S., Marstein, E. S. and Cremades, A., "Hybrid Materials and Nanoparticles for Hybrid Silicon Solar Cells and Li-Ion Batteries," *J. Energy Power Technol.* 2021, Vol. 3, Page 1 3(2), 1–1 (2021).
- [5] Ghosh, S., Maiyalagan, T. and Basu, R. N., "Nanostructured conducting polymers for energy applications: Towards a sustainable platform," *Nanoscale* 8(13), 6921–6947 (2016).
- [6] Gueye, M. N., Carella, A., Faure-Vincent, J., Demadrille, R. and Simonato, J. P., "Progress in understanding structure and transport properties of PEDOT-based materials: A critical review," *Prog. Mater. Sci.* 108, 100616 (2020).
- [7] Wang, S., Kang, Y., Wang, L., Zhang, H., Wang, Y. and Wang, Y., "Organic/inorganic hybrid sensors: A review," *Sensors Actuators, B Chem.* 182, 467–481 (2013).
- [8] Vázquez-López, A., Yaseen, A., Maestre, D., Ramírez-Castellanos, J., Marstein, E. S., Karazhanov, S. Z. and Cremades, A., "Synergetic Improvement of Stability and Conductivity of Hybrid Composites formed by PEDOT:PSS and SnO Nanoparticles," *Molecules* 25(3), 695 (2020).
- [9] Vázquez-López, A., Maestre, D., Ramírez-Castellanos, J., González-Calbet, J. M., Pis, I., Nappini, S., Yuca, N. and Cremades, A., "Influence of Doping and Controlled Sn Charge State on the Properties and Performance of SnO<sub>2</sub> Nanoparticles as Anodes in Li-Ion Batteries," *J. Phys. Chem. C* 124, 18490–18501 (2020).
- [10] Vázquez-López, A., Maestre, D., Ramírez-Castellanos, J. and Cremades, A., "In Situ Local Oxidation of SnO

Induced by Laser Irradiation: A Stability Study,” *Nanomaterials* 11(4), 976 (2021).

- [11] Vázquez-López, A., Yaseen, A., Maestre, D., Ramírez-Castellanos, J., Karazhanov, S. Z., Marstein, E. S. and Cremades, A., “Improved silicon surface passivation by hybrid composites formed by PEDOT:PSS with anatase TiO<sub>2</sub> nanoparticles,” *Mater. Lett.* 271, 127802 (2020).
- [12] Shi, H., Liu, C., Jiang, Q. and Xu, J., “Effective Approaches to Improve the Electrical Conductivity of PEDOT:PSS: A Review,” *Adv. Electron. Mater.* 1(4), 1–16 (2015).
- [13] Horcas, I., Fernández, R., Gómez-Rodríguez, J. M., Colchero, J., Gómez-Herrero, J. and Baro, A. M., “WSXM: A software for scanning probe microscopy and a tool for nanotechnology,” *Rev. Sci. Instrum.* 78(1), 013705 (2007).
- [14] Taeño, M., Maestre, D. and Cremades, A., “Fabrication and study of self-assembled NiO surface networks assisted by Sn doping,” *J. Alloys Compd.* 827 (2020).
- [15] Pasha, A., Khasim, S., Al-Hartomy, O. A., Lakshmi, M. and Manjunatha, K. G., “Highly sensitive ethylene glycol-doped PEDOT-PSS organic thin films for LPG sensing,” *RSC Adv.* 8(32), 18074–18083 (2018).
- [16] Cui, H. Q., Peng, R. X., Song, W., Zhang, J. F., Huang, J. M., Zhu, L. Q. and Ge, Z. Y., “Optimization of Ethylene Glycol Doped PEDOT:PSS Transparent Electrodes for Flexible Organic Solar Cells by Drop-coating Method,” *Chinese J. Polym. Sci. (English Ed.)* 37(8), 760–766 (2019).
- [17] Jäckle, S., Liebhaber, M., Niederhausen, J., Büchele, M., Félix, R., Wilks, R. G., Bär, M., Lips, K. and Christiansen, S., “Unveiling the Hybrid n-Si/PEDOT:PSS Interface,” *ACS Appl. Mater. Interfaces* 8(13), 8841–8848 (2016).
- [18] Khang, D. Y., “Recent progress in Si-PEDOT:PSS inorganic-organic hybrid solar cells,” *J. Phys. D. Appl. Phys.* 52(50), 503002 (2019).
- [19] Liu, Q., Ishikawa, R., Funada, S., Ohki, T., Ueno, K. and Shirai, H., “Highly Efficient Solution-Processed Poly(3,4-ethylenedioxythiophene):Poly(styrenesulfonate)/Crystalline-Silicon Heterojunction Solar Cells with Improved Light-Induced Stability,” *Adv. Energy Mater.* 5(17), 1500744 (2015).
- [20] Ziaur, M., Shahidul, R. • and Khan, I., “Advances in surface passivation of c-Si solar cells,” *Mater. Renew. Sustain. Energy* 2012 11 1(1), 1–11 (2012).
- [21] Kaloyeros, A. E., Pan, Y., Goff, J. and Arkles, B., “Review—Silicon Nitride and Silicon Nitride-Rich Thin Film Technologies: State-of-the-Art Processing Technologies, Properties, and Applications,” *ECS J. Solid State Sci. Technol.* 9(6), 063006 (2020).
- [22] García-Carrión, M., Ramírez-Castellanos, J., Nogales, E., Méndez, B., You, C. C., Karazhanov, S. and Marstein, E. S., “Hybrid solar cells with  $\beta$ - and  $\gamma$ - gallium oxide nanoparticles,” *Mater. Lett.* 261, 127088 (2020).
- [23] Dong, J., Gerlach, D., Koutsogiannis, P., Rudolf, P. and Portale, G., “Boosting the Thermoelectric Properties of PEDOT:PSS via Low-Impact Deposition of Tin Oxide Nanoparticles,” *Adv. Electron. Mater.* 7(5), 2001284 (2021).
- [24] Pasha, A., Khasim, S., Khan, F. A. and Dhananjaya, N., “Fabrication of gas sensor device using poly (3, 4-ethylenedioxythiophene)-poly (styrenesulfonate)-doped reduced graphene oxide organic thin films for detection of ammonia gas at room temperature,” *Iran. Polym. J. (English Ed.)* 28(3), 183–192 (2019).
- [25] Wang, C., Yin, L., Zhang, L., Xiang, D. and Gao, R., “Metal oxide gas sensors: Sensitivity and influencing factors,” *Sensors* 10(3), 2088–2106 (2010).
- [26] Wang, S., Kang, Y., Wang, L., Zhang, H., Wang, Y. and Wang, Y., “Organic/inorganic hybrid sensors: A review,” *Sensors Actuators, B Chem.* 182, 467–481 (2013).
- [27] Liu, Y. and Yang, Y., “Recent Progress of TiO<sub>2</sub>-Based Anodes for Li Ion Batteries,” *J. Nanomater.* 4, 1–15 (2016).
- [28] Dalapati, G. K., Sharma, H., Guchhait, A., Chakrabarty, N., Bamola, P., Liu, Q., Saianand, G., Sai Krishna, A. M., Mukhopadhyay, S., Dey, A., Wong, T. K. S., Zhuk, S., Ghosh, S., Chakraborty, S., Mahata, C., Biring, S.,



- Kumar, A., Ribeiro, C. S., Ramakrishna, S., et al., "Tin oxide for optoelectronic, photovoltaic and energy storage devices: a review," *J. Mater. Chem. A* 9(31), 16621–16684 (2021).
- [29] Li, T., Yuan, X.-Z., Zhang, L., Song, D., Shi, K., Bock, C. "Degradation Mechanisms and Mitigation Strategies of Nickel-Rich NMC-Based Lithium-Ion Batteries". *Electrochemical Energy Reviews*, 3, 43-80 (2020).
- [30] Xu, J., Lin, F., Doeff, M.M., Tong, W. "A review of Ni-based layered oxides for rechargeable Li-ion batteries," *J. Mater. Chem. A*, 5, 874–901, (2017).
- [31] Ruther, R. E., Callender, A. F., Zhou, H., Martha, S.K., Nanda, J. "Raman Microscopy of Lithium-Manganese-Rich Transition Metal Oxide Cathodes," *J. Electrochem. Soc.*, 162, A98–A102 (2015)

[\\*dmaestre@ucm.es](mailto:*dmaestre@ucm.es) ; phone: (+34) 913944495) ; <https://www.ucm.es/fine>